

*Original Research*

# Estimating Carbon Emissions in Urban Residential Areas by the Integration of Nighttime Lighting Intensity and Grid-based Fine-Grained Land Use Characteristics

**Qinxiang Wang, Haiyang Yu\*, Yundi Wang, Yuqing Cao**

School of Mathematical Sciences, Chengdu University of Technology, Chengdu 610059, China

*Received: 28 January 2025*

*Accepted: 25 March 2025*

## Abstract

China's residential energy consumption has been rising due to the country's fast urbanization and economic development. As a result, the precise measurement of residential carbon dioxide emissions (CE) is crucial for reducing greenhouse gas emissions and can serve as a foundation for the adoption of carbon reduction laws in urban areas. The purpose of this work is to develop a method that integrates fine-grained features of land use on a grid and nighttime light intensity (NLI) to estimate urban residential CE. First, the population and nighttime lighting data are used to depict the fine-grained land use features; second, three different unmixing models are built to obtain the NLIs of various land use types as well as the lighting values of residential areas; and third, the residential CE was estimated using the method of integrating NLI with the fine-grained land use features of the grid, and a comparative test was conducted. The study's findings indicate that (1) there is a strong positive linear association between the total amount of lights in residential areas and the residential CE of Guangzhou inhabitants, with a fitted  $R^2$  of 0.9318 at a 95% confidence probability. (2) From 2014 to 2022, Guangzhou residents' residential CE clearly displayed a growing tendency and a more pronounced clustering effect. (3) Residential CE can be estimated more accurately and precisely reflect the differences between different locations when it is based on fine-grained land use features and NLI. On the other hand, some residential regions' residential CE may be overestimated in the contrasting spatial visualization results, which are less likely to accurately reflect the variability of high CE locations (CE more than 2131t). The research findings can provide a solid database for future investigations, assisting the departments in developing more detailed environmental management and differentiation plans.

**Keywords:** residential carbon emissions, unmixing model, fine-grained land use characteristics, nighttime light intensity, spatial visualization

## Introduction

The World Meteorological Organization (WMO) publishes the Global Greenhouse Gas Bulletin, which indicates that in 2022, the annual average global atmospheric concentration of major greenhouse gases reached a new high, with the concentration of carbon dioxide (CO<sub>2</sub>) at 417.9±0.2 ppm, 150% of the pre-industrial (before 1750) level. The environment in which humans live is seriously threatened by the greenhouse effect [1]. The primary source of anthropogenic greenhouse gas (GHG) emissions is the combustion of fossil fuels, which accounts for over 70% of global GHG emissions [2]. Energy is typically used by a variety of consumer entities, such as retail, transportation, industry, agriculture, and residential use. Of these, residential energy use and carbon dioxide emissions make up a sizable portion of the global total for both energy consumption and emissions. According to statistics, residential direct energy consumption constituted 21% of global direct energy consumption [3]. As one of the greatest contributors to national CO<sub>2</sub> emissions in China, the residential sector is responsible for over 12.95% of the country's total energy consumption and is just behind the industrial sector (66.75%) [4]. However, if we divide energy consumption based on its final attribution, the proportion of energy consumption in the residential sector will far exceed that of other sectors. This is a critical area for China to meet its carbon peaking and carbon neutrality strategic goals. Additionally, it is anticipated that CO<sub>2</sub> emissions from residential home consumption will continue to rise as urbanization and industrialization continue [5]. Consequently, in order to effectively manage carbon emissions and solve climate change challenges, research on carbon emissions from residential living energy use is crucial.

Residential carbon emissions are the results of direct energy use, such as lighting, cooking, using electrical appliances, heating a home, and other activities that are directly associated with residential dwelling. The complexity of statistical data, variations in household energy consumption, and diversity in living energy consumption structures have made it harder to account for and restrict the spatial visualization of residents' residential carbon emissions and direct living energy consumption. In the meantime, the majority of research that has been done so far has focused on accounting for and spatially visualizing residents' carbon emissions at the provincial, municipal, county, functional area, and street block levels [6-10]. In terms of methodology, the input-output modeling approach, sectoral method, energy balance sheet method, and carbon emission coefficient method are frequently employed to account for residential carbon emissions [11-14].

The availability of spatial data, such as images from remote sensing, has given rise to fresh approaches to estimating carbon emissions. These include the use of

remote sensing images of nighttime lights that depict human activity on Earth's surface to measure a variety of socioeconomic statistics, and numerous studies have demonstrated a strong correlation between nighttime lights and carbon emissions [15-17]. These images can be utilized for carbon emission estimation analysis and spatial visualization [18-20], as well as for the high-precision spatial pattern of carbon emissions at the grid scale using DMSP/OLS data. For instance, Ghosh et al. created global CO<sub>2</sub> grid data from fossil fuel burning using DMSP/OLS evening lighting data [21]. They precisely separated national-scale CO<sub>2</sub> emissions into spatial grids of intermediate resolution by combining population grids with nighttime lighting images. In order to accurately define grid-scale CEs, Wu et al. suggested a technique for measuring CEs utilizing nighttime light data. Their method is more suited for long-term, large-scale carbon emissions monitoring and successfully makes up for the drawbacks of the conventional "bottom-up" statistical methodology [22]. Nevertheless, research on calculating the carbon emissions from direct residence energy usage and its spatial distribution using data on night lighting is lacking. In the Pearl River Delta (PRD) urban agglomerations, Wang et al. estimated the carbon emissions from residential energy consumption in the PRD urban agglomerations based on the spatial distribution of the resident population, which they obtained using a linear relationship between the total value of nighttime lighting and the resident population [23]. Zhao simulated settlement density using spatial data (DNVI and DEM imagery, DMSP/OLS nighttime lighting data) and then used that data as a carbon emission weight to obtain the spatial distribution pattern of carbon emissions from residential dwellings at a resolution of 1 km×1 km [24]. The majority of the aforementioned studies concentrate on applying the total nighttime lighting values of larger regions independently. They then use linear correlation to derive the carbon emission lighting coefficients for these regions, enabling the realization of spatial visualization and carbon emission estimation at the provincial, city, county, and functional area scales. Broadly speaking, issues include inadequate fine-grained analysis of illumination and carbon emissions in the area, challenges in accurately measuring carbon emissions from residential regions, and a dearth of studies on the spatial depiction of carbon emissions from residential areas.

Land use is a major source of anthropogenic carbon emissions and a driver of climate change, and higher-resolution land use data offer the possibility of refining carbon emissions within regions. Currently, there are more studies on carbon emissions from different land use types (e.g., forests, water, and wetlands) [25, 26], which have enriched the study of carbon emissions from land use at different spatial scales. In addition, some scholars have further studied the carbon emissions of all land use types. Zhang et al. analyzed the carbon emissions of the Yellow River Delta in 2000 based on

the data of land use types (farmland, forest land, grassland, wetland, watershed, construction land and unused land) and fossil energy consumption data during the same time period by constructing carbon emission models, carbon footprints, and Moran's I indices, and analyzed the spatial and temporal distribution characteristics of carbon emissions in the Yellow River Delta from 2000-2019 spatial and temporal distribution characteristics of carbon emissions in the Yellow River Delta [27]. Wang et al. divided the city based on the main road network, then classified it into 14 effective land use categories (agriculture, transportation, retail trade, residential, etc.) based on land use functions and land cover composition, and finally measured the relationship between land use and carbon emissions [28]. In addition, land use is also an important determinant of nighttime light from a physical point of view [29]. Li et al. developed a model to quantify the contribution of land use to nighttime light using coarse-resolution nighttime light images and fine-resolution land use data [30]. In light of this, integrating land use and nighttime light data to achieve a fine-grained analysis of urban residential carbon emissions is an innovative exploration that holds significant value for Chinese cities seeking to accelerate the attainment of carbon neutrality and carbon peak by adopting appropriate carbon emission control measures that are tailored to community needs.

The objective of this paper is to develop a technique for calculating urban residential carbon emissions by incorporating fine-grained features of land use on a grid and nighttime light intensity (NLI). Additionally, the study aims to offer a high-resolution spatial visualization and an accurate estimate of Guangzhou City's residential carbon emissions for the years 2014-2022. The main contributions of this paper are summarized as follows: (1) The average nighttime light intensities of different land use types estimated by three types of unmixing models (non-negative least squares model, non-negative spatial lag model, and non-negative spatial error model) are compared, and the evaluation standard is the reference NLI, which is computed from the nighttime light data of Luojial-01. (2) To reflect the variations in NLI and minimize the error between the estimated and true NLI values for each grid, fine-grained characteristics based on population data and nighttime lighting were assigned to different grids within the same land use category. (3) The mixed light values of each grid were separated into residential and non-residential light values using an ideal unmixing model that integrated NLI and fine-grained land use features from the grid. (4) In order to determine the spatial distribution pattern of carbon emissions of residential areas in Guangzhou, a linear fitting model was developed between the light values of residential areas and the carbon emissions of residential areas derived from statistical data. The estimated carbon emissions were assigned to each 500 m×500 m grid.

## Framework

This paper proposes a method for estimating urban residential carbon emissions by integrating grid land use fine-grained features and NLI, and takes Guangzhou City as an example to refine the estimation and spatial visualization of its residential carbon emissions from 2014 to 2022, and the research framework is shown in Fig. 1. The specific steps are as follows:

Step 1: Three models are built to fit the nighttime light and land use based on the unmixing technique. Using these models, it is achievable to determine the NLIs of various land use categories and to differentiate between residential and non-residential lights.

Step 2: To reduce the error produced by the unmixing model, which uses the NLIs as homogenous global variables to solve, combine the population data and nighttime light data to assign fine-grained features to the land use of each grid.

Step 3: Compare the estimation accuracies of the three unmixing models based on the reference NLIs calculated from the higher resolution lighting data.

Step 4: Using Guangzhou City as an example, the best unmixing model with integrated grid land use fine-grained features and NLIs is used to estimate the lighting values of its residential areas, and linearly fitted to the carbon accounting data, to obtain the estimated value of carbon emissions from residential dwellings as well as the spatial distribution pattern of carbon emissions.

Step 5: Without taking into account the specifics of the land use of the grid, compute the spatial distribution of carbon emissions from urban residential sources in greater detail and compare the results with the study findings presented in this paper.

## Study Area

Guangzhou City (22°26'-23°56'N, 112°57'-114°3'E) is located in the southern part of Guangdong Province, with a total area of 7,434.40 km<sup>2</sup>, including Liwan, Yuexiu, Haizhu, Tianhe, Baiyun, Huangpu, Panyu, Huadu, Nansha, Conghua, and Zengcheng, a total of 11 administrative districts (Fig. 2). Guangzhou, the biggest city in southern China, has developed over the years into a major hub for foreign political, economic, and cultural contacts in southern China as well as an international business hub with significant worldwide radiation power. Estimating, analyzing, and spatially visualizing urban residents' carbon emissions over time is theoretically significant. The study's findings can help residents adopt low-carbon consumption and living practices, as well as serve as a theoretical foundation for Guangzhou's low-carbon city's development and related decision-making.

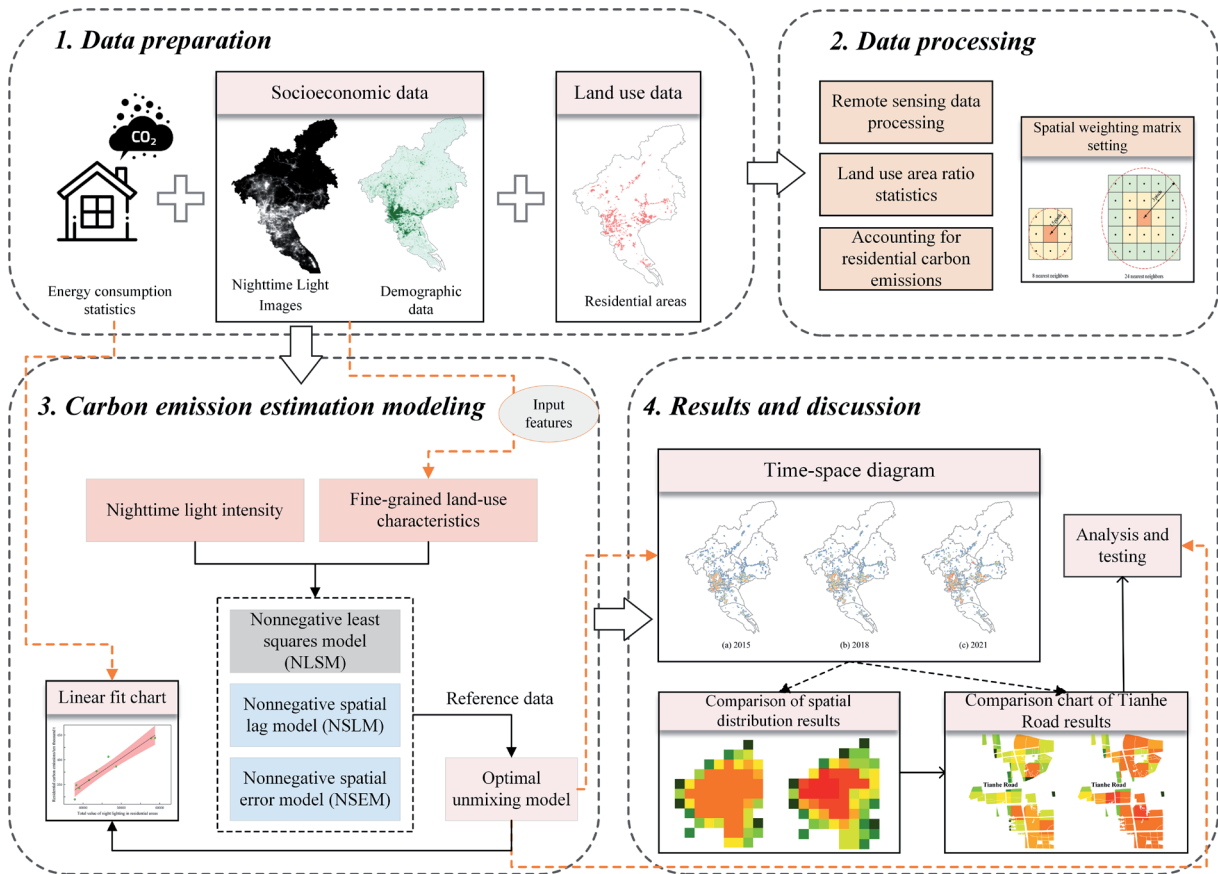


Fig. 1. Research framework diagram.

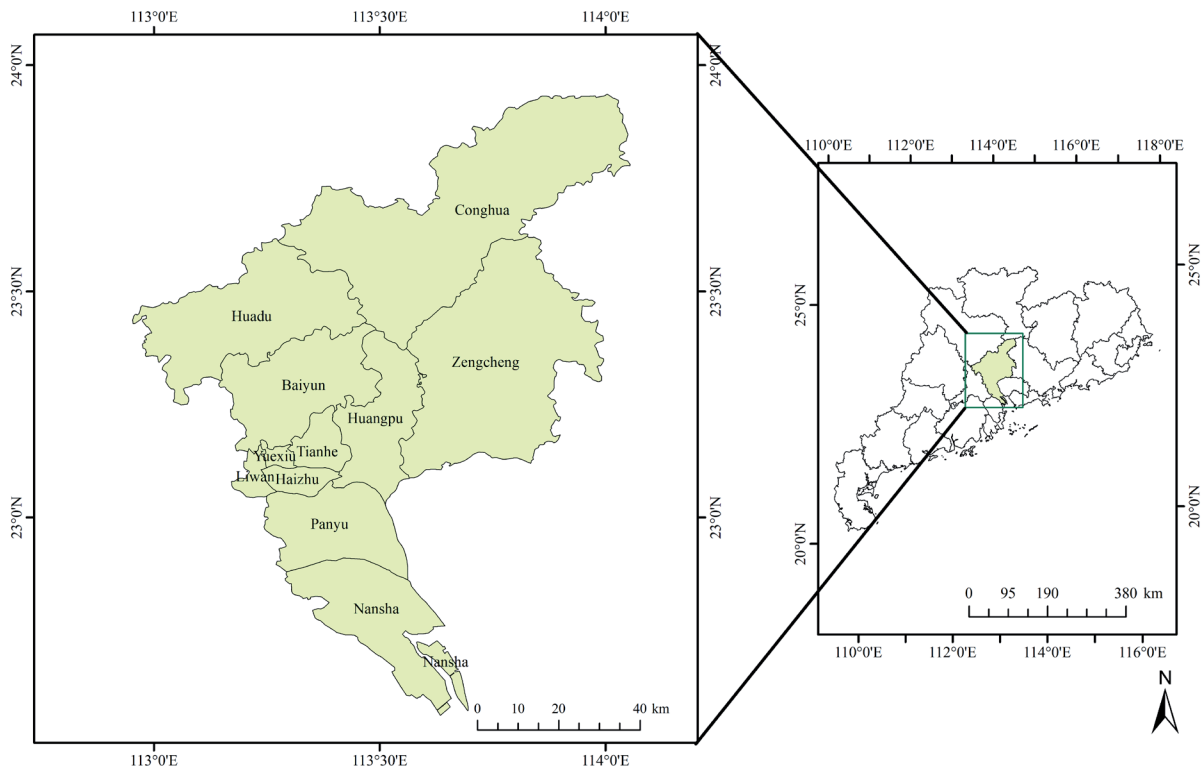


Fig. 2. Geographic location of the study area.

Table 1. Details of the data used in this study.

Data name	Data description	Time	Sources
Composite product of NPP/VIIRS	Nighttime light data with a spatial resolution of 500 m	2014-2022	EOG, Colorado School of Mines
		26/10/2018	
Luojia1-01	Nighttime light data with a spatial resolution of 130 m	26/10/2018	High Resolution Earth Observation System, <a href="http://www.hbeos.org.cn/">http://www.hbeos.org.cn/</a>
EULUC-China	Data on basic urban land-use types in China with a spatial resolution of 30 m	2018	Department of Earth System Science, Tsinghua University
Demographic data	Raster data on the distribution of the resident population with a spatial resolution of 1 km	2014-2022	LandScan platform developed by the U.S. Department of Energy's Oak Ridge National Laboratory (ORNL)
Guangzhou Energy Consumption Data	Domestic Energy Consumption Data by Species in Guangzhou	2014-2022	Guangzhou Municipal Bureau of Statistics

### Data Sources

Table 1 below shows the details of the data used in this paper, including two types of NTL data: the Composite product of NPP/VIIRS and Luojia1-01, land use data (EULUC-China), population data, and energy consumption data for Guangzhou.

### Data Processing

#### Remote Sensing Data Processing

The original Composite product of NPP/VIIRS nighttime images used in this paper is from the annual global nighttime product produced by the Earth Observation Group (EOG) based on nighttime Diurnal Night Band (DNB) microluminescence imaging data collected by the NASA/NOAA Visible Infrared Imaging Radiometer Suite (VIIRS). Its data provider radiometrically corrects the nighttime images and removes background noise [31]. Therefore, the projection transformation and resampling of this nighttime image was performed directly to avoid distortion of the image grid with latitude. Secondly, the Luojia1-01 night light

data were radiometrically corrected as well as denoised [32, 33], in which the radiometric correction formula for Luojia1-01 product is as follows:

$$L = DN^{3/2} \times 10^{-10} \quad (1)$$

where L is the radiance brightness value after absolute radiance correction and DN is the image gray value. Finally, in order to ensure the uniformity of the resolution of remote sensing data, this paper uses the nearest neighbor method to resample the population raster data to 500m.

#### Spatial Weighting Matrix Setting

The non-negative spatial lag model (NSLM) and the non-negative spatial error model (NSEM) [34] will be built in the next section to represent the spatial autocorrelation effect between the grid's lighting values. Furthermore, the regression outcomes for these two kinds of spatial autoregressive models are significantly impacted by the spatial weight matrix W that is established [35]. As illustrated in Fig. 3 below, two k values (k = 8 and k = 24) are ultimately chosen

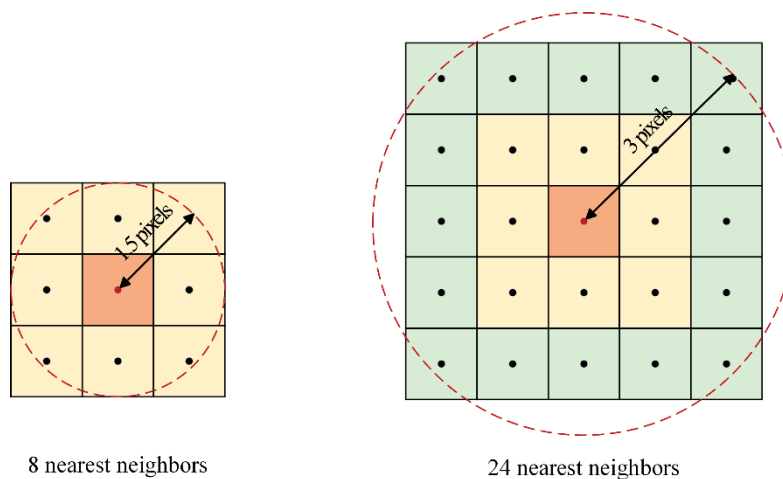


Fig. 3. Spatial weight matrix setup.

as the influence range of spatial autocorrelation affecting features, which correspond to the thresholds of 1.5 and 3 image elements, respectively, based on the studies that have already been conducted [34]. The weights of the grids in the adjacent area of the center grid are set to the inverse of their distances, and the weights of the rest of the grids are set to zero.

#### Land Use Type Area Ratio Statistics

The majority of grids contain mixed land types because of the resolution difference between land use maps and images of nighttime light. However, only a small number of land types exist in a given grid because of the geographic autocorrelation of land use. The unmixing technique assumes that each grid's nighttime light may be represented as a linear combination of land use areas, and each land use type's average nighttime light intensity is utilized as a coefficient [30]. Consequently, this study computes the proportion of each land use type's area in each grid.

#### Accounting for Residential Carbon Emissions

This paper utilizes the carbon emission coefficient method to carry out a preliminary accounting of residential carbon emissions in Guangzhou from 2014 to 2022, and the carbon emission coefficients of each energy source refer to the Greenhouse Gas Emission Inventory 2006 issued by IPCC, as shown in Table 2 below. The calculation formula of the reference method is as follows:

$$C = \sum_i (AD_i \times EF_i) \quad (2)$$

Where  $C$  denotes carbon emissions,  $AD_i$  denotes the total amount of energy consumed by sub-species in the residential sector, kg of standard coal, and  $EF_i$  denotes the emission factor of sub-species of energy in the residential sector, kg/kg of standard coal.

## Method

### Unmixing Model

Land use is a significant physical factor that influences nighttime light [29]. On the other hand, nighttime light images have a coarser spatial resolution than regular land use maps. Because different land use types are mixed in the coarse resolution grid of the

nighttime light imagery, making it difficult to determine the light intensity in residential areas, the resolution gap makes it more difficult to use land use maps (EULUC-China) to obtain accurate nighttime light values for land use types in residential areas. Hence, this paper will build three types of unmixing models to obtain the NLIs of different land use types as well as the light values for residential areas. This will help to distinguish between residential and non-residential lights that are mixed in the same grid and to obtain more accurate nighttime light values for residential areas.

#### Nonnegative Least Squares Model (NLSM)

Based on the unmixing strategy, it is assumed that the nighttime light of each grid can be expressed as a linear combination of land use areas, and the average nighttime luminescence of land use type  $i$  is used as a coefficient denoted as  $a_i$ , i.e., nighttime light intensity (NLI). For the land area representable by the available grid  $j$ , there are  $n$  potential land use types with area proportions  $\{x_{j1}, \dots, x_{jm}\}$ , and the satellite-recorded nighttime light values for this grid are denoted as  $y_j$ . Therefore, the following linear model is constructed to fit the nighttime light and land use [30]:

$$\begin{cases} y_1 = a_1x_{11} + \dots + a_mx_{1m} + \varepsilon_1 \\ y_2 = a_1x_{21} + \dots + a_mx_{2m} + \varepsilon_2 \\ \dots \\ y_n = a_1x_{n1} + \dots + a_mx_{nm} + \varepsilon_n \end{cases} \quad (3)$$

where  $\varepsilon_j$  denotes the model error for grid  $j$  and  $n$  denotes the total number of grids, i.e., the number of observations of the model. The model can also be rewritten in the following matrix form:

$$Y = Xa + \varepsilon \quad (4)$$

According to the physical meaning, the land use brightness coefficient  $a_i$  should be non-negative, therefore, the model can be solved by the constrained least squares algorithm [36].

#### Nonnegative Spatial Autoregressive Model

The aforementioned non-negative least squares model models each grid's light brightness using the land use area share, but it ignores the impact of the neighboring grids. Furthermore, multispectral remote sensing images and nighttime light remote sensing data

Table 2. Carbon emission factors by energy source.

	Raw coal	Gasoline	Kerosene	Diesel	Electrical power	Petroleum
Carbon emission factor/(kgC/kgce)	0.75590	0.55380	0.57140	0.59210	0.27200	0.44830

will show spectral dependency between neighboring pixels, or spatial autocorrelation, as a result of sensor resolution and terrain heterogeneity [37]. Thus, while examining the relationship between night light data and land use data, the spatial autocorrelation effect between light data should be taken into account. Using previous research as a guide, two different kinds of spatial autoregressive models are built in this work [34].

#### Nonnegative Spatial Lag Model (NSLM)

The light emitted from objects inside the pixel may affect the brightness of the surrounding pixels through photorefracton and reflection, reflecting the fact that the lighting value of a particular grid is not only affected by its own explanatory variables, but also by the lights of the other surrounding grids, and thus a spatial lag model (SLM) can be constructed as follows:

$$Y = \rho WY + X\beta + \varepsilon, \varepsilon \sim N[0, \sigma^2 I] \quad (5)$$

where  $Y$  is the matrix of nighttime light values,  $X$  is the matrix of area proportions,  $\beta$  is the vector of average nighttime light intensities, and  $\beta_0$  is assumed to be non-negative based on physical significance.  $\rho$  is the coefficient of the  $WY$  term of the spatial lag model, which takes a value in the range of (0, 1).  $W$  is the spatial weight matrix, which denotes the influence between all grid pairs in the space, and  $\varepsilon$  denotes the vector of normally distributed random errors.

For the above SLM model, the known data is  $(X, Y)$ , and the unknown parameter is  $\theta = (\beta, \rho, \sigma^2)$ , deforming the model by

$$(I_n - \rho W)Y - X\beta = \varepsilon \quad (6)$$

The log-likelihood function of the vector  $\theta$  can be obtained based on the condition that  $\varepsilon$  follows a normal distribution:

$$\ln L = \ln |I_n - \rho W| - \frac{n}{2} \ln(2\pi\sigma^2) - \frac{1}{2\sigma^2} [(I_n - \rho W)Y - X\beta]' [(I_n - \rho W)Y - X\beta] \quad (7)$$

The estimation method of the traditional spatial lag model is to use the first-order condition of  $\beta, \sigma^2$  to get the log-likelihood function of parameter  $\rho$ , and then use various optimization methods to solve the great value of the log-likelihood function of parameter  $\rho$ , so as to get the estimated values of the coefficients. The SLM model set in this paper adds a non-negative constraint on parameter  $\beta$ , so the estimation method of the traditional spatial lag model is not applicable. Considering the scale of the data and the boundary constraint requirement in this paper, the log-likelihood function of Eq. (7)

is optimized using the L-BFGS-B algorithm to obtain the estimated value of  $\beta$  under the non-negative constraint. Numerical experiments have demonstrated the effectiveness of the L-BFGS-B algorithm [38] in solving large-scale variable bounded constraint optimization problems. The algorithm was developed from the BFGS algorithm, a proposed Newtonian algorithm with constraints. The objective function and its gradient  $g$  vector are all that are required to be provided throughout the optimization solution process; the Hessian matrix need not be computed.

#### Nonnegative Spatial Error Model (NSEM)

Spatial autocorrelation is also caused by the effects of climatic and atmospheric conditions, positive correlations caused by imaging systems, etc., which suggests that there are spatial perturbation terms and overall spatial correlations in addition to the effects of the dependent variable, and that perturbations in a given space affect other spaces with spatial effects, and thus a spatial error model (SEM) can be constructed as follows:

$$\begin{aligned} Y &= X\beta + \varepsilon \\ \varepsilon &= \lambda W\varepsilon + u, u \sim N[0, \sigma^2 I] \end{aligned} \quad (8)$$

where  $\lambda$  is the spatial error correlation coefficient with a value in the range of (0, 1).  $W$  is the spatial weight matrix indicating the effect of residuals in the space, and  $u$  is the normally distributed random error vector.

Similarly, for the above SEM model, the unknown parameter is  $\tau = (\beta, \lambda, \sigma^2)$ , and the known data is  $(X, Y)$ . Appropriate deformations of the model have:

$$\begin{aligned} Y &= X\beta + \lambda Wu + \varepsilon, \\ Y - \lambda WY &= (X - \lambda WX)\beta + \varepsilon, \end{aligned} \quad (9)$$

Let  $Y_\lambda = Y - \lambda WY, X_\lambda = X - \lambda WX$ , then  $Y_\lambda - X_\lambda\beta = \varepsilon$ , so the log-likelihood function of the vector  $\tau$  is:

$$\ln L = \log |I_n - \lambda W| - \frac{n}{2} \ln(2\pi\sigma^2) - \frac{1}{2\sigma^2} (Y_\lambda - X_\lambda\beta)' (Y_\lambda - X_\lambda\beta) \quad (10)$$

The traditional estimation method of the spatial error model is to use the first-order condition of  $\beta, \sigma^2$  to write Eq. (10) as an explicit expression about  $\lambda$ , and then solve  $\lambda$  to maximize the log-likelihood function about  $\lambda$ . In this paper, the model requires the parameter  $\beta$  to be non-negative, and the traditional estimation method is not applicable, so the L-BFGS-B algorithm is also used to optimize Eq. (10) to obtain the optimal non-negative estimation value of the parameter  $\beta$ .

### Fine-Grained Features

The aforementioned unmixing models all solve for NLIs as homogeneous global variables, which raises the risk of significant errors in both the residential nighttime lighting values computed from NLIs and the true values for each grid, as well as between the estimated and true NLIs. The NLIs of different land use types and socioeconomic characteristics are closely related, and there are some variances in the NLIs of the same land use type in different grids [39]. To assign fine-grained land use characteristics to each grid, this article, therefore, integrates the population data with the nighttime light data.

Due to its straightforward premise and great interpretability, the K-means algorithm is a classic clustering technique that has seen extensive use [40]. It can realize the grouping of geographic areas and effectively identify the fine-grained features of each group, so in this paper, the nighttime lighting data and population data are used as the input features of K-means clustering, and the clustering categories obtained from K-means clustering are used as the fine-grained features of the grid land use. The basic idea of the K-means clustering algorithm is to randomly select K data objects from a dataset as the initial centers, calculate the distance of each data object to each center, divide all data objects into clusters located in the center closest to it according to the nearest neighbor principle, and then recalculate the data mean value in each cluster as the new clustering center for the next iteration. The sum of squared errors (SSE) within the clusters is continuously reduced until the clustering center no longer changes or the objective function converges when the clustering stops [41]. The determination of the K value in the K-means clustering algorithm has a large impact on the clustering results, and in this paper, we choose the elbow method to select the optimal number of clusters. In order to find the optimal number of clusters, this paper combines the K value obtained by the elbow method to complete the first clustering, and then according to the situation in the group after clustering to determine whether to carry out fine clustering on certain subsets to improve the accuracy of the clustering results.

### Estimation of Carbon Emissions

This paper is able to create the unmixing model for each clustering category independently by taking into account the fine-grained characteristics of the grid's land use. It is well known that the total brightness values of all land use types, which are obtained by multiplying the NLI of each land use type by its proportion of area in the center grid, can be used to indicate the nighttime lighting value of a grid within each clustering subregion. Consequently, each grid's lighting values on each clustered sub-area are precisely assigned to the residential areas on it using the unmixing model and the following formula:

$$ResDN_j = P_j \times NLI_j \quad (11)$$

Where  $ResDN_j$  refers to the residential area light value of grid j,  $P_j$  is the residential area proportion of grid j, and  $NLI_j$  is the residential area nighttime light intensity of grid j. As a result, the residential area light value of each 500 m×500 m grid can be obtained. Next, a fitting model of carbon emissions from urban residents' domestic energy consumption and total nighttime lighting values of residential areas is established. Numerous methods have been used to model the spatial pattern of socioeconomic data using nighttime light data, such as linear regression models, log-log regression models, and second-order regression models. Among these methods, linear regression models are relatively accurate and easy to implement [42]. Therefore, this study still uses a linear regression model to estimate residential carbon emission [43]:

$$C_0 = a_0 \times TDN + b_0 \quad (12)$$

$$\alpha = \frac{C_0}{TDN} \quad (13)$$

Where  $C_0$  is the corrected residential carbon emission,  $a_0$  and  $b_0$  are the regression coefficient and intercept,  $TDN$  is the total value of residential lights, and  $\alpha$  is the carbon emission allocation factor. Finally, based on the allocation principle that carbon emissions are positively correlated with the DN values of lights at night, the carbon emissions from residential housing in each grid can be obtained by multiplying  $ResDN_j$  by the coefficient  $\alpha$ , and the spatial distribution pattern of carbon emissions from residential housing with a resolution of 500 m×500 m is obtained.

## Results and Discussion

### Comparison of Unmixing Model Performance

This research uses linear regression to evaluate the relationship between the estimated values of NLI for land use types in Guangzhou generated from the aforementioned three models and the reference NLI values in order to assess the estimation accuracy of the three unmixing models. The data used in the unmixing model is the Composite product of NPP/VIIRS nighttime lighting data on the day of 2018.10.26, and the reference data is the 130m resolution Luojia1-01 nighttime lighting data on the same day. To guarantee the correctness of the reference NLI data, a lower resolution land use scale map is first created from the original land use map because the resolution of the reference nighttime light data is still lower than that of the land use data. The average nighttime light for each land use type is then obtained as the reference NLI value by gathering all

Table 3. R<sup>2</sup> of linearly fitted NLI values for the three models at different distance thresholds.

Study area	Distance threshold				
	/	7.5 km			1.5 km
Guangzhou City	NLS	NSLM	NSEM	NSLM	NSEM
	0.93626	0.93634	0.93633	0.93652	0.93659

of the grids that are fully occupied by a specific land use type, which are referred to as pure grids. The results of the three models' linear regression fitting are displayed in the Table 3. A higher goodness of fit indicates improved estimation accuracy and a better capacity to capture the relationship between land use type and NLI [26]. As can be observed, the best accuracy of the estimated value of NLI derived from the building of the non-negative spatial error model is achieved when the threshold value of the spatial weight matrix is set to 3 pixels, and the fitted model's R<sup>2</sup> reaches 0.93659. Therefore, in order to estimate the value of the lights in Guangzhou City's residential area, a non-negative spatial error model will be built in the next part.

#### Estimation of Residential Carbon Emissions in Guangzhou

The accurate nighttime lighting values of residential areas in Guangzhou City from 2014 to 2022 were obtained using the non-negative spatial error model with integrated grid land use granularity and nighttime lighting intensity. These values were then linearly fitted to the carbon emission accounting data above. The fitting equations are displayed in the following equation, and the fitting relationship is displayed in Fig. 4 below:

$$C_0 = 0.00528 \times TDN + 138.76881 \quad (14)$$

The results show that the carbon emissions from the domestic energy consumption of Guangzhou residents have a good positive linear correlation with the total value of lighting in residential areas, with a goodness of fit of 0.9318 at 95% confidence probability.

#### Spatial Visualization of Residential Carbon Emissions in Guangzhou City

Based on the fitting coefficients of the above linear model and the nighttime lighting values of the grid residential areas, the corrected total residential carbon emissions of Guangzhou City for the calendar year are assigned to each grid, which is calculated as follows:

$$C_{(i)(j)} = \alpha_i \times ResDN_{(i)(j)} \quad (15)$$

where  $C_{(i)(j)}$  is the carbon emission from domestic energy consumption of the  $j$ th grid in year  $i$ ,  $\alpha_i$  is the carbon emission allocation factor in year  $i$ , and  $ResDN_{(i)(j)}$  is the lighting value of the residential area of the  $j$ th grid in year  $i$ . The spatial distribution pattern of residential carbon emissions in Guangzhou City is derived through the use of ArcGIS's spatial analysis and statistics. Fig. 5 displays the spatial distribution maps of carbon emissions in the years 2015, 2018, and 2021. The findings can be used to display Guangzhou's residential carbon emissions' temporal

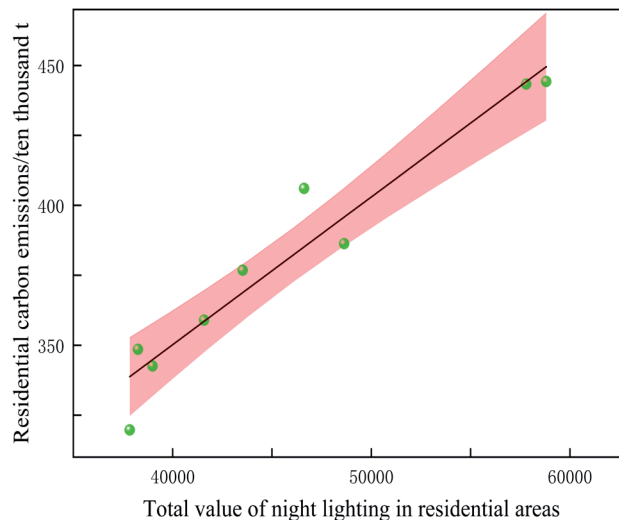


Fig. 4. Fitted relationship between residential carbon emissions and total value of lights in residential areas.

and spatial distribution characteristics: (i) From 2014 to 2022, there was a clear upward trend in Guangzhou's residential carbon emissions. The city's main urban areas, including the districts of Baiyun, Tianhe, Yuexiu, Liwan, and Haizhu, as well as the peripheral districts of Zengcheng and Panyu, had greater growth and eventually became the center of the city's high residential carbon emissions. (ii) From 2014 to 2022, Guangzhou's residential carbon emissions gap both within and between districts progressively widened, demonstrating a more pronounced aggregation effect. There could be a number of reasons for this, including the unequal development of regional livelihoods, the absence of population and industrial agglomeration potential in periphery urban regions, and the uneven level of regional economic development in Guangzhou. (iii) Guangzhou City's residential carbon emissions gradually exhibit a geographical pattern that stretches along the eastward direction from the heart of the main metropolitan region as the city actively responds to the "eastward" plan. In particular, the eastern regions of Guangzhou-Huangpu District and Zengcheng District – have much higher residential carbon emissions in 2021 compared to 2015.

This research further explores the spatial distribution of household carbon emissions in Guangzhou in 2021, as shown in Fig. 6 below, in order to better explore the spatial distribution of residential carbon emissions in Guangzhou. Overall, it appears that there is a dispersed pattern of residential carbon emissions decreasing from the inner city to the outlying area. Residential carbon emissions in the central city of Guangzhou are all at a high level, among which, the residential areas in Baiyun and Tianhe districts generally have higher carbon emissions due to the fact that their resident

populations are among the top, with obvious population aggregation effects, and their young people account for a higher proportion of the population, with more frequent economic activities. Yuexiu District has the highest degree of population aging, and its residential carbon emissions are generally only at a medium level, which is lower than those of the remaining major urban areas. After many years of construction, the eastern part of the district, with Huangpu and Zengcheng District as the main parts, has already become the industrial core agglomeration of Guangzhou. This is closely related to Guangzhou's urban spatial development strategy of developing along the Pearl River to the east. Among the peripheral urban areas, the residential areas in Huangpu District and the southwestern part of Zengcheng District also have high carbon emissions.

### Spatial Visualization Data Analysis and Examination of Carbon Emissions

In order to reflect the influence of grid land use fine-grained features on the results of spatial visualization of residential carbon emissions in Guangzhou, this paper further calculates the results of the spatial distribution of residential carbon emissions in Guangzhou in 2018 without clustering, and compares and tests the results of the above studies in this paper with the same year. In contrast, this paper combines the grid land use fine-grained features to more effectively reflect the differences between different geographic regions and more finely reflect the pattern of residential carbon emissions within the city, as shown in Fig. 7 – Fig. 10. There is a discrepancy in the residential carbon emissions of residents in residential districts even in

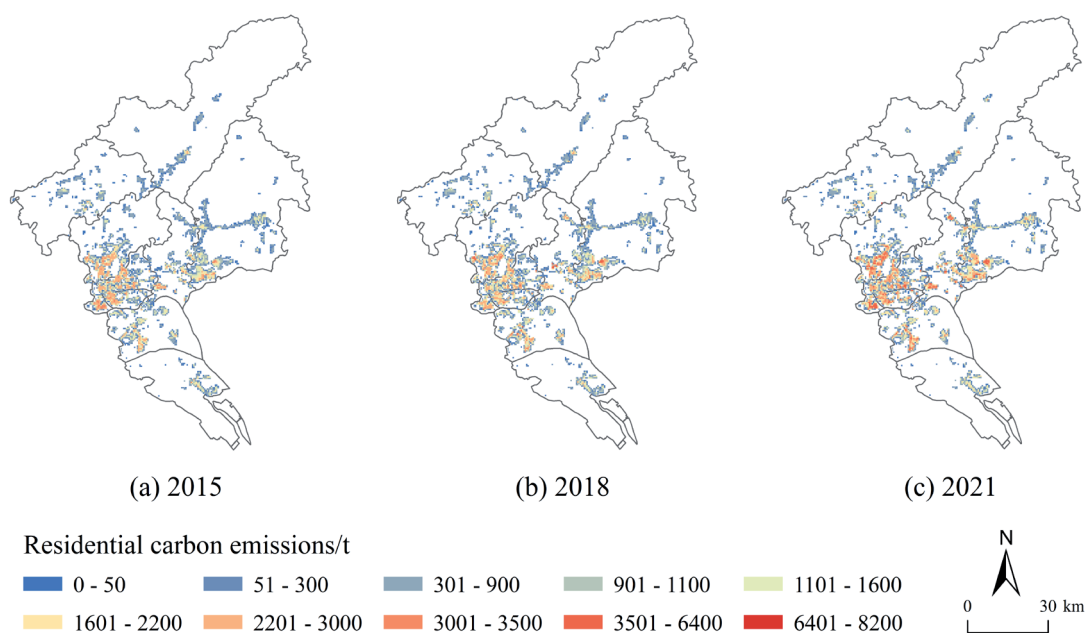


Fig. 5. Spatial distribution of residential carbon emissions in Guangzhou City.

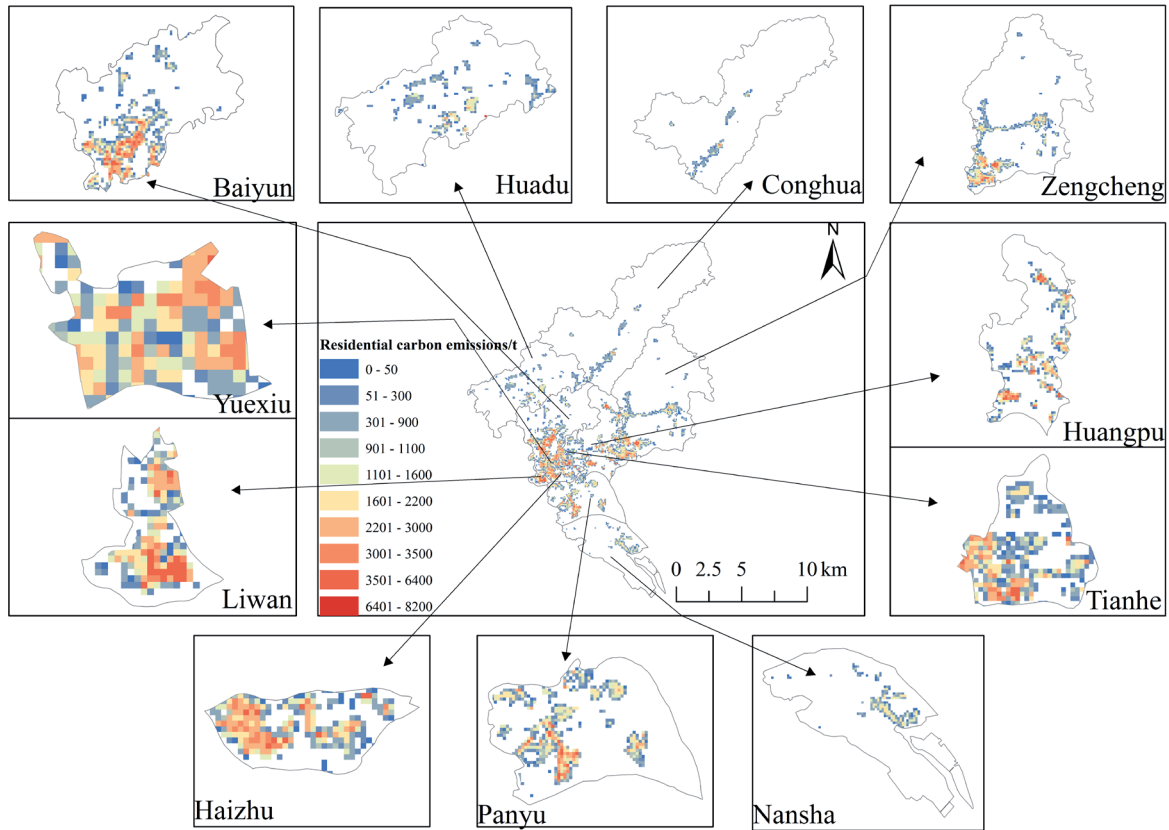


Fig. 6. Spatial distribution of residential carbon emissions in Guangzhou in 2021.

neighboring regions because factors like the income, consumption, and energy structures of residents have specific effects on residential carbon emissions. As can be seen from Fig. 7, the spatial visualization results of (a) are more difficult to reflect the differences in high carbon emission areas (carbon emissions greater than 2131t), in contrast, the spatial visualization results

of (b) reflect the differences and contrasts at a finer scale, thus better reflecting the specific influence of specific factors on residential carbon emissions, and helping the relevant departments to formulate a fine-grained environmental management and control strategy and establish differentiated low-carbon consumption patterns.

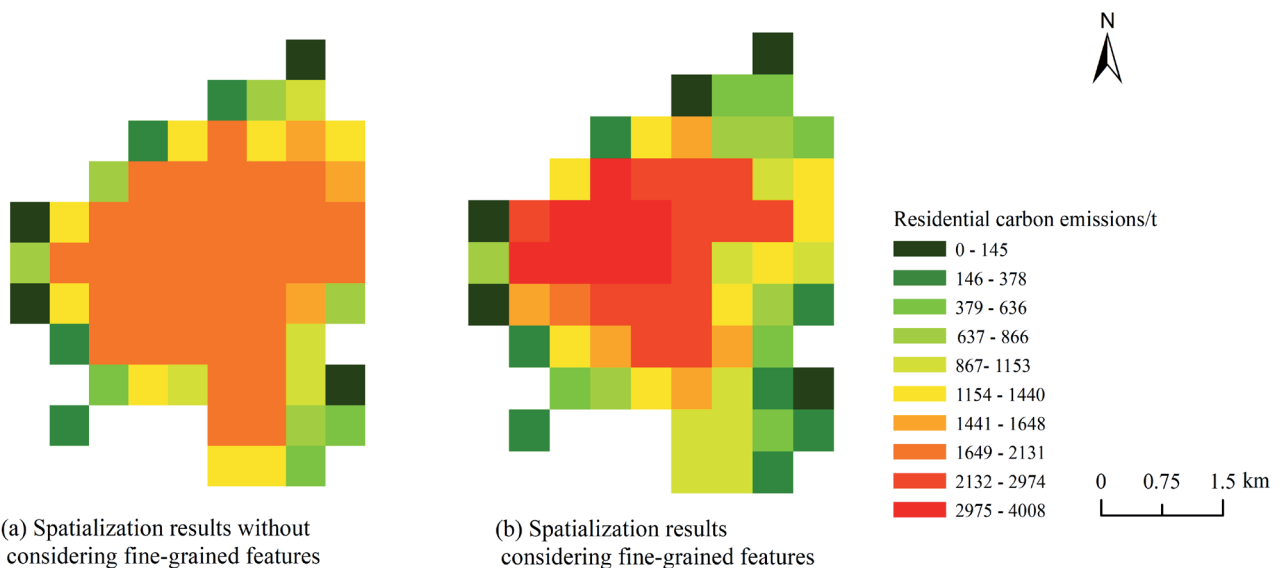


Fig. 7. Comparison of the results of spatial distribution of residential carbon emissions in Guangzhou City in 2018.

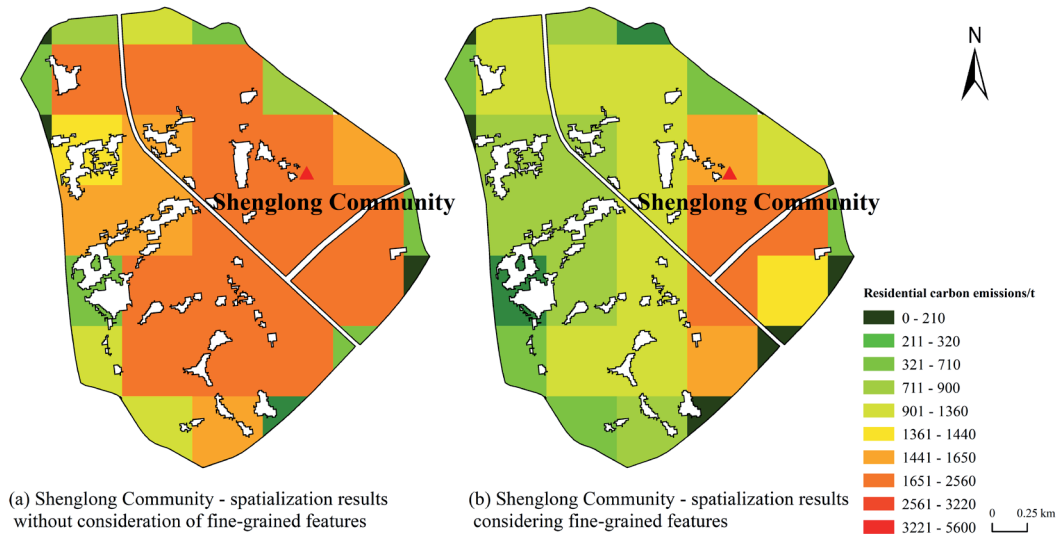


Fig. 8. Comparison of the results of spatial distribution of residential carbon emissions in Shenglong Community.

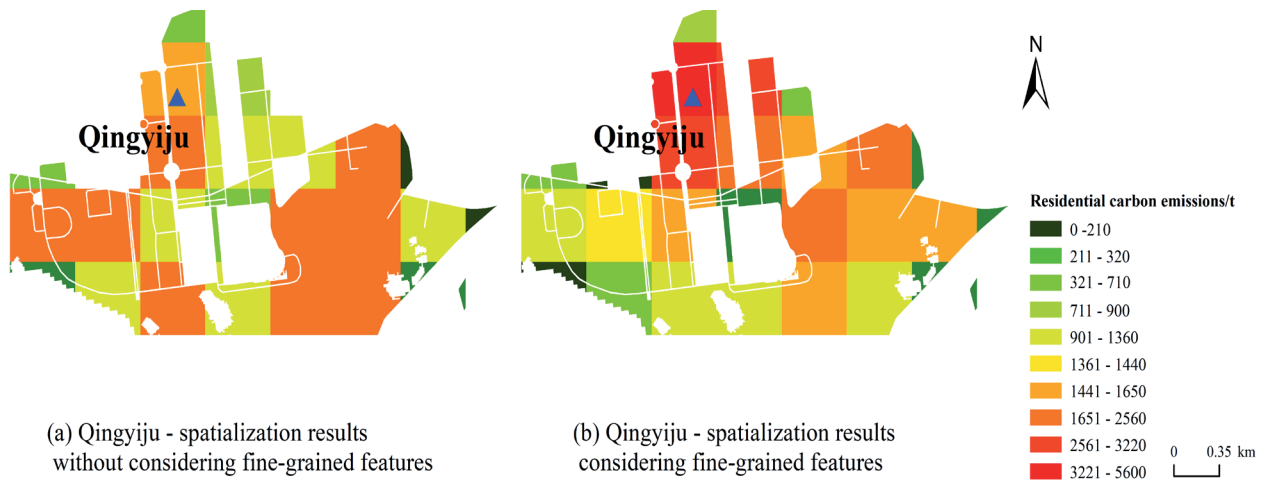


Fig. 9. Comparison of the results of the spatial distribution of residential carbon emissions of Qingyiju residents.

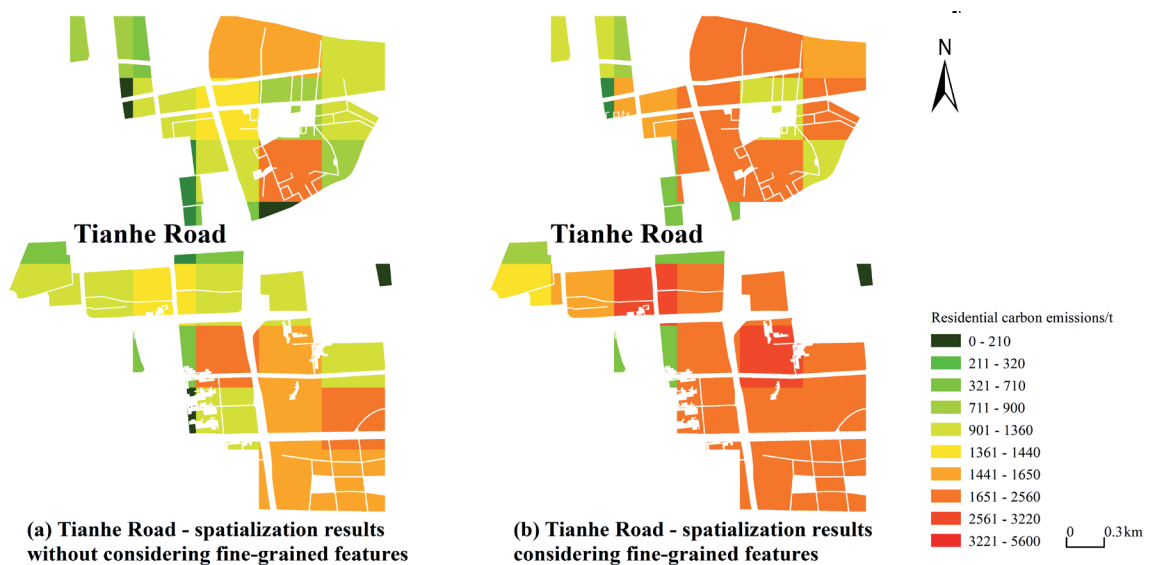


Fig. 10. Comparison of the results of spatial distribution of carbon emissions from residential housing on Tianhe Road.

Specifically, Fig. 8 shows the results of the comparison of the spatial distribution of residential carbon emissions in Shenglong Community, which is located in Hualong Town, Panyu District, Guangzhou City, and is a multi-year-old community, with an overall more dilapidated community environment and various basic facilities and lower housing prices. Secondly, the residential buildings in Shenglong Community are lower in height and more sparsely distributed, and there are few recreational facilities around it. Shenglong Community is located in a large industrial town in the Panyu District, and the population density of residential areas in the community is low. As a result, the level of its residential carbon emissions is generally low. Fig. 8(a) overestimates its residential carbon emissions, while Fig. 8(b) captures the differentiated characteristics of carbon emissions from residential areas in the Shenglong Community well. Fig. 9 shows the comparative results of the carbon emission distribution of the residents of Qingyiju, which is located in Panyu District, Guangzhou City, in the new village of Qifu. The village is known as “the first village in China” for its international cultural community with a large environment, large facilities and large transportation. Qingyiju is located in the vicinity of the commercial plaza, and its residential buildings are of medium height, with a large base area, dense distribution, and high population density. Therefore, the residential carbon emission level of Qingyiju is generally higher. Compared with Fig. 9(a), the residential carbon emission level of Qingyiju in Fig. 9(b) is higher than 3200t, which accurately identifies the residential area with high residential carbon emission. Fig. 10 shows the comparative results of the distribution of carbon emissions from residential areas near Tianhe Road, which is located on the new central axis of Guangzhou and is the core business district of Guangzhou, with the reputation of “the first golden business belt in South China”. As the leading consumer in Guangzhou, the Tianhe Road business district has frequent economic activities and high population density and is one of the areas with high carbon emissions in the center of Guangzhou. As a result, the residential carbon emissions from the residential areas in its neighborhood are generally at a high level, and the carbon emission results in Fig. 10(b) accurately reflect the high level of residential carbon emissions from the residential areas in the neighborhood of the Tianhe Road business district. The aforementioned findings demonstrate how this paper’s research method of estimating urban residential carbon emissions by integrating fine-grained land use and nighttime light intensity can more accurately simulate the spatial distribution of carbon emissions in residential areas and highlight variations in residential carbon emissions in small-scale areas. This information can then be used to inform decisions about land use, resource allocation, and urban management that relate to the control of carbon emissions from urban residential areas.

## Conclusion

Numerous studies have demonstrated that nighttime light images captured by remote sensing technology can offer distinctive viewpoints and methods for observing and analyzing nocturnal human activity. This paper integrates fine-grained features of land use on a grid and nighttime light intensity to study the carbon emissions and spatial distribution of residential carbon emissions in urban residential areas. Compared with previous studies on carbon emissions based on nighttime lighting data, this paper focuses on land use, which is an important factor in determining nighttime lighting. Despite the fact that prior studies have mostly shown that combining data from many remote sensing sources (including land use, POI, population density, and nighttime lights) has a high ability to estimate carbon dioxide emissions [44, 45], they are frequently concentrated at bigger scales, including the national, provincial, municipal, and street block levels, and primarily concentrate on total carbon emissions [6, 46, 47]. However, the findings of this paper’s spatial distribution of carbon emissions can serve as a crucial foundation for breaking down urban emission reduction targets into residential sub-regions. This makes it easier to develop and execute targeted emission reduction strategies in each area based on the local circumstances. Furthermore, it is very difficult to estimate the emissions of different forms of carbon dioxide and visualize them visually because of the unequal spatial distribution of these emissions. While several studies have produced high-resolution residential carbon emission maps using nighttime light data [48, 43], they failed to take into account the mixed presence of various carbon emission types inside the pixels. However, the model developed in this paper effectively allocated household carbon emissions to finer spatial units (500 m×500 m) using multi-source data, and our methods significantly improved the timeliness and accuracy of CE simulation ( $R^2 = 0.9318$ ), with results better than those reported in previous studies of the same type ( $R^2 = 0.7668$ ) [43].

In particular, Guangzhou City’s example study was started by this work. First, the unmixing model was built to quantify the contribution of land features to the nighttime lighting, taking into account the resolution gap between the land use data and the nighttime lighting data. Next, the mixed lighting values of the grids were classified into residential and non-residential lighting. Second, the light and population data are used to provide a fine-grained characterization of the variations in NLIs within the same land use type across grids, hence improving the limits of the unmixing model to solve for NLIs as a homogenous global variable. Finally, the fitting model between the residential carbon emissions accounted for by the statistical data and the total value of residential lighting is established to obtain the corrected total residential carbon emissions and the spatial distribution map of carbon emissions

in Guangzhou City, which is analyzed and examined, and the main conclusions are as follows:

(1) Comparing the estimates of NLIs obtained from the three unmixing models with the reference NLIs values, it was concluded that the estimates of NLIs obtained from the construction of the non-negative spatial error model had the highest accuracy when the threshold of the spatial weight matrix was set to 3 pixels, and the fitted model  $R^2$  reached 0.93659.

(2) The results of the constructed linear fitting model indicate a good positive linear correlation between residential carbon emissions and the total lighting value of residential areas in Guangzhou, with a goodness-of-fit of 0.9318 at 95% confidence probability.

(3) The findings from the spatial visualization of Guangzhou's residential carbon emissions indicate that, between 2014 and 2022, the city's residential carbon emissions showed a significant growth trend, with the main urban areas and the peripheral districts' Zengcheng and Panyu districts showing the greatest growth. In addition, the gap in residential carbon emissions within and between Guangzhou City's districts from 2014 to 2022 gradually widened, indicating a more pronounced aggregation effect; in 2021, Guangzhou's residential carbon emissions as a whole displayed a spatial pattern of dispersion from the central urban area to the surrounding area.

(4) Residential CE can be more accurately estimated and more accurately reflect regional variations at a finer scale when it is based on the finer-grained characteristics of land use and nighttime light intensity. By contrast, when comparing the spatial visualization findings, it is easy to exaggerate the carbon emissions from residential areas and difficult to portray the differences between locations with large carbon emissions (carbon emissions greater than 2131t).

This work builds an unmixing model to replicate the spatial distribution pattern of residential carbon emissions, which might serve as a database for future studies. In addition, a high-resolution map of the distribution of residential carbon emissions will give policymakers additional insights to meet emission reduction targets while also assisting different departments in developing more specialized low-carbon consumption patterns and fine-grained environmental management and control strategies. However, there are still some issues with this paper. For instance, errors will inevitably occur due to the availability of statistical data, inconsistent statistical calibre, and other factors. This paper only establishes a simple linear fitting model between the carbon emissions of residential housing and the value of lighting in residential districts, and the results obtained have certain errors. Taking into account the data problem and the significance of Guangzhou City, this paper only uses Guangzhou City, a first-tier city, as the research object, which has a smaller research scope. Other types of cities are also included in the research scope, which better indicates the model's universality.

To improve the generalizability of the carbon emission estimating model, this work will subsequently widen the study region and consider the remaining elements affecting carbon emissions in residential areas.

### Acknowledgements

I want to thank Dr. Yu for guidance in my research. Our conversations inspired me to write the entire work and complete it successfully. He always made me feel confident in my skills and guided me to many important publications that were quite helpful.

Conceptualization: Wang, Q.X.; Methodology, Wang, Q.X.; Software, Wang, Q.X. and Wang, Y.D.; Formal Analysis, Wang, Q.X. and Cao, Y.Q.; Investigation, Cao, Y.Q.; Resources, Yu, H.Y.; Writing – Original Draft Preparation, Wang, Q.X.; Writing – Review & Editing, Yu, H.Y. and Wang, Y.D.; Visualization, Cao, Y.Q.; Project Administration, Yu, H.Y.

### Conflict of Interest

The authors declare no conflicts of interest.

### References

1. LI C., LI H., QIN X. Spatial heterogeneity of carbon emissions and its influencing factors in China: evidence from 286 prefecture-level cities. *International Journal of Environmental Research and Public Health*, **19** (3), 1226, **2022**.
2. INTERGOVERNMENTAL PANEL ON CLIMATE CHANGE. *Climate Change 2007: Mitigation: Contribution of Working Group III to the Fourth Assessment Report of the IPCC*. Cambridge University Press: Cambridge, UK, **2007** [In English].
3. CHEN P., JIANG R., CHEN Z.M. Global household energy consumption structure: direct versus embodied perspective from 2000 to 2014. *Energy, Ecology and Environment*, **9** (1), 100, **2024**.
4. BEI L., YANG W., WANG B., GAO Y., WANG A., LU T., LIU H.T., SUN L.S. Characteristics of residents' carbon emission and driving factors for carbon peaking: A case study in Wuhan, China. *Energy for Sustainable Development*, **81**, 101471, **2024**.
5. NEJAT P., JOMEHZADEH F., MAHDI M., GOHARI M., MAJID M. A global review of energy consumption, CO<sub>2</sub> emissions and policy in the residential sector (with an overview of the top ten CO<sub>2</sub> emitting countries). *Renewable and Sustainable Energy Reviews*, **43**, 843, **2015**.
6. ZHENG Y.S., LI W.J., JIANG L., YUAN C., XIAO T., WANG R., CAI M., HONG H.B. Spatial modelling of street-level carbon emissions with multi-source open data: A case study of Guangzhou. *Urban Climate*, **55**, **2024**.
7. GAO J., LIU H., TANG Y., LUO M. Hybrid method of mapping urban residential carbon emissions with high-spatial resolution: A case study of Suzhou, China. *Environment and Planning B: Urban Analytics and City Science*, **51** (1), 75, **2024**.

8. WANG J., YOU K., QI L., REN H. Gravity center change of carbon emissions in Chinese residential building sector: Differences between urban and rural area. *Energy Reports*, **8**, 10644, **2022**.
9. YANG X., SIMA Y., LV Y., LI M. Research on influencing factors of residential building carbon emissions and carbon peak: A case of Henan province in China. *Sustainability*, **15n**(13), 10243, **2023**.
10. YANG L., ZHANG X.L. Study on Measurement and Influencing Factors of Household Carbon Emission in Jiangsu Province: An Empirical Analysis Based on GTWR Model. *Ecological Economy*, **36** (5), 31, **2020** [In Chinese].
11. ZHANG Y.J., BIAN X.J., TAN W., SONG J. The indirect energy consumption and CO<sub>2</sub> emission caused by household consumption in China: an analysis based on the input–output method. *Journal of Cleaner Production*, **163**, 69, **2017**.
12. FAN J.S. ZHOU L. A comparative study on the changes of residential living consumption carbon emissions in urban and rural China. *China Environmental Science*, **38** (11), 4369, **2018** [In Chinese].
13. YANG Y., JIA J., CHEN C. Residential energy-related CO<sub>2</sub> emissions in China's less developed regions: A case study of Jiangxi. *Sustainability*, **12** (5), 2000, **2020**.
14. FENG D., YAN C. Driving factors and decoupling analysis of carbon emissions from energy consumption in high energy-consuming regions: a case study of Liaoning province. *Frontiers in Environmental Science*, **12**, 1406754, **2024**.
15. DOLL C.H., MULLER J.P., ELVIDGE C.D. Night-time imagery as a tool for global mapping of socioeconomic parameters and greenhouse gas emissions. *AMBIO: a Journal of the Human Environment*, **29** (3), 157, **2000**.
16. ELVIDGE C.D., IMHOFF M.L., BAUGH K.E., HOBSON V.R., NELSON I., SAFRAN J., DIETZ J.B., TUTTLE B.T. Night time lights of the world: 1994-1995. *ISPRS Journal of Photogrammetry and Remote Sensing*, **56** (2), 81, **2001**.
17. ZUO C., GONG W., GAO Z., KONG D., WEI R., MA X. Correlation analysis of CO<sub>2</sub> concentration based on DMSP-OLS and NPP-VIIRS integrated data. *Remote Sensing*, **14** (17), 4181, **2022**.
18. WU K., WANG X. Aligning pixel values of DMSP and VIIRS nighttime light images to evaluate urban dynamics. *Remote Sensing*, **11** (12), 1463, **2019**.
19. ODA T., ROMÁN M.O., WANG Z., STOKES E.C., SUN Q., SHRESTHA R.M., FENG S., LAUVAUX T., BUN R., MAKSYUTOV S. US Cities in the Dark: Mapping Man-Made Carbon Dioxide Emissions Over the Contiguous US Using NASA's Black Marble Nighttime Lights Product. *Urban Remote Sensing: Monitoring, Synthesis, and Modeling in the Urban Environment*, 337, **2021**.
20. FERRADA G.A., ZHOU M., WANG J., LYAPUSTIN A., WANG Y.J., FREITAS S.R., CARMICHAEL G.R. Introducing the VIIRS-based fire emission inventory version 0 (VFEIv0). *Geoscientific Model Development*, **15** (21), 8085, **2022**.
21. GHOSH T., ELVIDGE C.D., SUTTON P.C., KIMBERLY E.B., ZISKIN D., TUTTLE B.T. Creating a global grid of distributed fossil fuel CO<sub>2</sub> emissions from nighttime satellite imagery. *Energies*, **3** (12), 1895, **2010**.
22. WU H., YANG Y., LI W. Dynamic spatiotemporal evolution and spatial effect of carbon emissions in urban agglomerations based on nighttime light data. *Sustainable Cities and Society*, **113**, 105712, **2024**.
23. WANG Y.J., WANG M.J., LIU L., LI S., LIN Y. Analyzing the spatiotemporal differences of carbon emission in the Pearl River Delta using DMSP/OLS nighttime light images. *National Remote Sensing Bulletin*, **26** (9), 1824, **2022** [In Chinese].
24. ZHAO J.C. Simulation study of residential carbon emission model based on night lighting. Henan University: Henan, China, **2015** [In Chinese].
25. CARNELL P.E., WINDECKER S.M., BRENNER M., BALDOCK J., MASQUE P., BRUNT K., MACREADIE P.I. Carbon stocks, sequestration, and emissions of wetlands in south eastern Australia. *Global Change Biology*, **24** (9), 4173, **2018**.
26. RAJBANSHI J., DAS S. Changes in carbon stocks and its economic valuation under a changing land use pattern-A multitemporal study in Konar catchment, India. *Land Degradation & Development*, **32** (13), 3573, **2021**.
27. ZHANG C.Y., ZHAO L., ZHANG H., CHEN M., FANG R., YAO Y., ZHANG Q., WANG Q. Spatial-temporal characteristics of carbon emissions from land use change in Yellow River Delta region, China. *Ecological Indicators*, **136**, 108623, **2022**.
28. WANG G., HAN Q. Assessment of the relation between land use and carbon emission in Eindhoven, the Netherlands. *Journal of Environmental Management*, **247**, 413, **2019**.
29. KUECHLY H.U., KYBA C.C.M., RUHTZ T., LINDEMANN C., WOLTER C., FISCHER J., HÖLKER F. Aerial survey and spatial analysis of sources of light pollution in Berlin, Germany. *Remote Sensing of Environment*, **126**, 39, **2012**.
30. LI X., GE L., CHEN X. Quantifying contribution of land use types to nighttime light using an unmixing model. *IEEE Geoscience and Remote Sensing Letters*, **11** (10), 1667, **2014**.
31. ELVIDGE C.D., ZHIZHIN M., GHOSH T., TANEJA J. Annual time series of global VIIRS nighttime lights derived from monthly averages: 2012 to 2019. *Remote Sensing*, **13** (5), 922, **2021**.
32. ZHANG Y.X., LI X., SONG Y., LI C. Urban Spatial Form Analysis of GBA Based on "LJ1-01" Nighttime Light Remote Sensing Images. *Journal of Applied Sciences - Electronics and Information Engineering*, **23** (6), 1011, **2019**.
33. LIN Z.L., ZU H.Q., LIN C.H. Estimation of anthropogenic heat flux of Fujian Province (China) based on Luojial-01 nighttime light data. *Journal of Remote Sensing*, **2021**.
34. ZHENG H., GUI Z., WU H., SONG A. Developing non-negative spatial autoregressive models for better exploring relation between nighttime light images and land use types. *Remote Sensing*, **12** (5), 798, **2020**.
35. KELEJIAN H.H., PRUCHA I.R. A generalized spatial two-stage least squares procedure for estimating a spatial autoregressive model with autoregressive disturbances. *The Journal of Real Estate Finance and Economics*, **17**, 99, **1998**.
36. LAWSON C.L., HANSON R.J. Solving least squares problems. *Society for Industrial and Applied Mathematics*, **1995**.
37. CHEN D., WEI H. The effect of spatial autocorrelation and class proportion on the accuracy measures from different sampling designs. *ISPRS Journal of Photogrammetry and Remote Sensing*, **64** (2), 140, **2009**.
38. BYRD R.H., LU P., NOCEDAL J., ZHU C. A limited memory algorithm for bound constrained optimization. *SIAM Journal on Scientific Computing*, **16** (5), 1190, **1995**.

39. YUE W., WU T., LIU X., ZHANG L., WU C., YE Y., ZHENG G. Developing an urban sprawl index for China's mega-cities. *Acta Geographica Sinica*, **75** (12), 2730, **2020**.
40. FRÁNTI P., SIERANOJA S. How much can K-means be improved by using better initialization and repeats? *Pattern Recognition*, **93**, 95, **2019**.
41. LIU H.F., CHEN J.X., DY J., FU Y. Transforming complex problems into K-means solutions. *IEEE Transactions on Pattern Analysis and Machine Intelligence*, **45** (7), 9149, **2023**.
42. SHI K., YU B., HUANG Y., HU Y., YIN B., CHEN Z., CHEN L., WU J. Evaluating the ability of NPP-VIIRS nighttime light data to estimate the gross domestic product and the electric power consumption of China at multiple scales: A comparison with DMSP-OLS data. *Remote Sensing*, **6** (2), 1705, **2014**.
43. ZHAO J., CHEN Y., JI G., WANG Z. Residential carbon dioxide emissions at the urban scale for county-level cities in China: A comparative study of nighttime light data. *Journal of Cleaner Production*, **180**, 198, **2018**.
44. SHI K., YU B., ZHOU Y., CHEN Y., YANG C., CHEN Z., WU J. Spatiotemporal variations of CO<sub>2</sub> emissions and their impact factors in China: A comparative analysis between the provincial and prefectural levels. *Applied Energy*, **233**, 170, **2019**.
45. CHEN H., ZHANG X., WU R., CAI T. Revisiting the environmental Kuznets curve for city-level CO<sub>2</sub> emissions: based on corrected NPP-VIIRS nighttime light data in China. *Journal of Cleaner Production*, **268**, 121575, **2020**.
46. ZHANG X.Y., XIE Y.W., JIAO J.Z., ZHU W.Y., GUO Z.C., CAO X.Y., LIU J.M., XI G.L., WEI W. How to accurately assess the spatial distribution of energy CO<sub>2</sub> emissions? Based on POI and NPP-VIIRS comparison. *Journal of Cleaner Production*, **402**, **2023**.
47. PAN K.X., LI Y.F., ZHU H.X., DANG A.R. Spatial Configuration of Energy Consumption and Carbon Emissions of Shanghai, and Our Policy Suggestions. *Sustainability*, **9** (1), **2017**.
48. LU H.L., LIU G.F., MIAO C.H., ZHANG C.R., CUI Y.P., ZHAO J.C. Spatial pattern of residential carbon dioxide emissions in a rapidly urbanizing Chinese city and its mismatch effect. *Sustainability*, **10** (3), 827, **2018**.